AEM JOURNAL.ORG

Wind-storage Synergistic Rapid Frequency Response Technology Incorporating Frequency Security Characteristics

Jian Zhang
School of Electrical Engineering, Northeast Electric Power University, Jilin 132012, Jilin, China
Corresponding author: Jian Zhang (e-mail: 18147521230@163.com)

ABSTRACT Under the framework of dual-carbon goals, renewable-generation capacity in the power grid continues to increase, while the share of conventional synchronous units declines, reducing system rotational inertia and weakening frequency security. This study first evaluates inertia demand based on frequency-stability requirements and then analyzes the synthetic inertia capability of wind turbines and battery energy storage. An integrated frequency-response model incorporating virtual inertia from combined wind-storage systems is developed, and an energy-storage capacity allocation method is proposed considering wind speed, system frequency-security metrics (ROCOF, $\Delta f_{\max}$, Δf_{ss}), and wind-turbine operating constraints such as rotational-speed safety and power limits. Simulation results show that at low wind speeds, where turbines lack frequency-regulation capability, energy storage effectively raises the minimum frequency point and reduces ROCOF. At rated wind speed, combined wind-storage regulation significantly reduces ROCOF compared with standalone turbine regulation, with a simulated reduction of 39.9%, raises the lower frequency limit, and minimizes steady-state frequency deviation. The study provides a wind-storage integrated rapid frequency-response technology for improving electromagnetic transient stability in high-renewable power systems.

INDEX TERMS inertia demand, wind-storage coordinated control, virtual inertia, frequency response, electromagnetic transient stability

I. INTRODUCTION

Driven by relentless technological and industrial progress, worldwide energy consumption is rising steadily year by year. These developments have catalyzed significant growth in renewable energy technologies, primarily wind and solar power, whose share within the power grid has grown annually. Due to their random and unstable nature, these sources can readily cause various issues within the grid, including frequency security and stability [1–2]. As the electrical devices containing green power are non-spinning stationary parts, increasing their proportion and replacing traditional power generators reduces the network's overall rotational inertia. This lowers the maximum load capacity and harmonic distortion capacity of the power system. In severe cases, quick frequency changes may occur, and the speed and severity of voltage drops may trigger tertiary protection such as low-frequency load shedding [3].

Wind turbine generators (WTGs), particularly (DFIGs), possess a certain potential for frequency support. However, their inertia response often comes at the expense of operational economy [4]. And the design and coordination of control strategies still face numerous technical challenges. Existing research has explored various strategies for WTGs, this encompasses approaches like droop control, virtual inertia emulation, harnessing kinetic energy stored in rotors, and assistance from capacitor-based energy storage, with the objective of mimicking the frequency response behaviors exhibited by synchronous generators [5–7].

Latency control, power recovery, multi-unit collaboration, and the collective response of the entire network all require further improvement. Adaptive fractional-order strategy to demonstrate a new adaptive fractional-order framework for frequency stabilisation, which is specifically designed for low-inertia environments and microgrids. This advanced method of grid frequency regulation uses a data-oriented approach and integrates inertia with droop mechanisms in DFIG [8]. In the study [9], in order to improve the utilisation of rotor kinetic energy in wind turbines and ensure the safe operation of rotors during design, an accurate prediction algorithm for rotor velocity is established using piecewise fitting and the Bernoulli equation. In addition, this way can achieve joint control of (BESS) and (SCESS), facilitating a smooth transition from grid-connected operation to autonomous mode for low-voltage microgrids that integrate wind turbines, photovoltaic modules, energy storage units, etc. [10]. Through the integrated management of WT rotor velocity and pitch angle regulation. (RSC) combines the suggested power-tracked deloads with frequency control signals, and (PAC) adjusts its logic in real time based on the rotational speed of the wind turbine (WT). Through such synchronisation, the plan has stored a fraction of the wind output in advance and will deploy it when there is a low-frequency situation.

The rapid development of machine learning suggests that power grids still have the potential for improvement in areas such as control delay, power recovery, multi-unit collaboration, and group-level system reactions at this stage. To address the unpredictability and fluctuations of wind energy, a wind farm generation prediction framework that integrates a density-based clustering optimizer using a density-based nearest neighbour search method with an ARIMA-LSTM ensemble architecture is proposed [11]. In research [12], phasor measurement units (PMUs) were employed to collect active energy and frequency data at the generator terminals. The generator's active generation output was used as the input of the data-centric model, and frequency deviations were taken as targets; A data-driven controlled autoregressive identification structure was built for the generator. Finally, using the diminishing memory recursive least squares method determined the grid's equivalent inertia.

The fast-tracking performance and stable-convergence characteristics assist in accurately calculating the rapidly changing equivalent virtual inertia of wind farms, and the online monitoring of the network's time-varying equivalent inertia during disturbances is also realised. The transient frequency dynamics of systems heavily reliant on renewable energy are a primary driver for the rapid evolution of modern power grid control technologies. Extending the traditional System Frequency Response (SFR) framework [13]. Governing synchronous motors. Variable power units for network frequency management have been appraised. Virtual synchronous machines have been introduced to emulate the inertia response and governor droop characteristics of synchronous units. Subsequently, a frequency response scheme for a multi-phase system with renewable energy was established, and it was converted into a typical single-machine model. This transformation enabled numerical optimisation by using equivalent summations [14]. Emphasizing the frequency valley of the power grid's dynamic response characteristics to separate the calculation of governor responses and frequency offsets. Finally, using a polynomial approximation to determine the fundamental frequency response characteristic at each stage [15].

In this context, the current study focuses on the frequency regulation technology of wind power grid-connected systems that have a high proportion of new energy. By evaluating offline the potential of wind and storage inertia reserves through operational limits, and by predicting disturbance reference power based on system inertia requirements, a wind-storage synergy-based rapid frequency response method is introduced to distribute virtual inertia among wind and storage units. A grid simulation framework for areas with high wind power penetration is then built. This indicates that the traditional generator and the wind-storage facility can achieve the objective of multiple sources' quickfrequency regulation under the proposed regulation plan, thereby meeting the system's frequency safety standard flexibly.

II. MATERIALS AND METHODS

A. A FREQUENCY RESPONSE MODEL FOR GRID INTEGRATION OF WIND-STORAGE

A feature of a power network is that it is less responsive to variations in rotor speed caused by disturbances outside the electrical system. To what extent the inertia is connected to the loss of stability of active power oscillations. A larger total rotational inertia of the grid is more sensitive to sudden changes in active power. In traditional power grids, conventional generators, such as hydroelectric and thermal power plants, primarily function to realise frequency regulation; these units possess substantial rotational inertia and regulatory capacity and jointly ensure the overall stability of the power system. However, due to the large-scale access of intermittent renewable energy sources such as wind power, these traditional frequency modulation resources have been displaced to a considerable extent, and the electrical network's inertia and regulation capability have dropped significantly.

The dynamic frequency behaviour of a power grid that is highly integrated with wind energy can be described using the SFR framework in terms of the contribution of wind farms to frequency regulation. The SFR framework developed in this study is composed of four integrated modules: (i) wind turbine system dynamics, (ii) conventional thermal power plant characteristics, (iii) power demand disturbance models, and (iv) underfrequency load shedding (UFLS) protocols. As illustrated in the control flow of Figure 1, each wind turbine utilizes vector control technology to independently regulate active and reactive power. In this simplified modeling approach, it can be considered that all wind-power generating units on a particular farm will be subject to identical working circumstances. Therefore, the operating deviations of each generator are not considered, and the total inertia parameter of the entire wind farm is obtained by summing up the inertia parameters of all individual units.

In modern power systems, wind turbines are often required to provide a certain frequency response capability, Integrated inertia control is a method for wind turbines to provide auxiliary FM, and the resulting additional power output is expressed as:

$$\Delta P_{\mathrm{we}} = -K_{\mathrm{WD}}\Delta f - K_{\mathrm{WI}}\frac{d\Delta f}{dt} \tag{1}$$

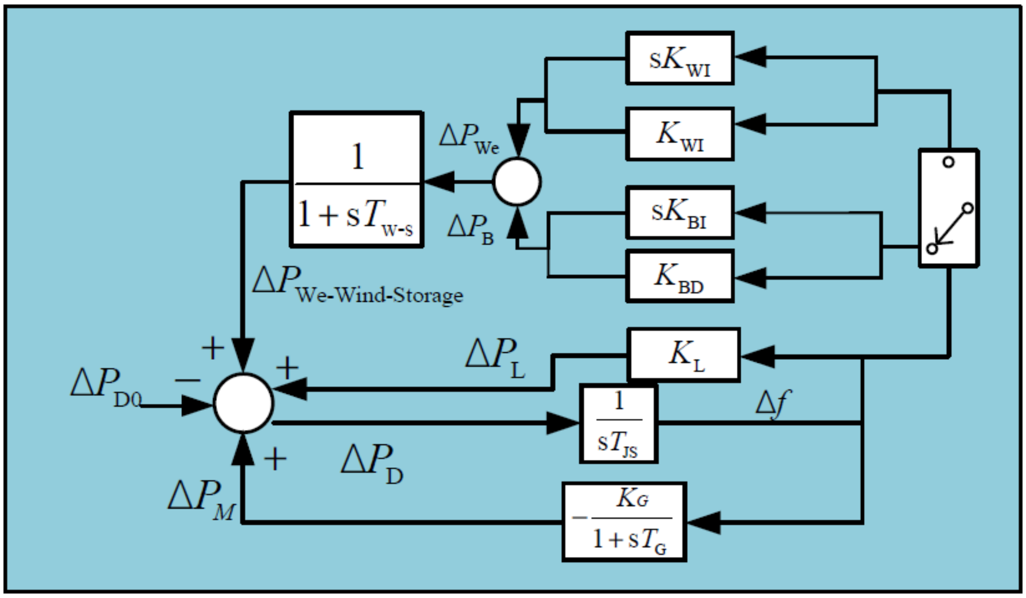

FIGURE 1. Modernized Power System Block Diagram of Simplified System

In the double-fed induction generator (MPPT) control mode, its contribution of inertia support to the power system is low. As a result, the total system inertia mainly depends on the synchronous generators. The sum of the active power changes, denoted as ΔP_{We}, is due to the fact that the MPPT method links the active energy production of the wind turbine to its rotor's angular velocity, so its reference output is essentially derived from the change in speed of the turbine.

$$\Delta P_{\mathrm{we}} = g(\omega_w) \tag{2}$$

The mechanical behaviour of the (WTG) rotor is described as follows: Subsequently, there are some equations; subsequently, it is subject to the following equation.

$$T_{\mathrm{JW}}\omega_w \frac{d\omega_w}{dt} = P_{\mathrm{wm}} - P_{\mathrm{we}} \tag{3}$$

Where, T_{JW} is the rotor inertia time constant of the WTG; P_{WM} represents the wind energy harvested by the turbine; and P_{WE} is the electrical power of the generator. Neglecting the pitch angle variation and assuming a stable wind speed WTG, the wind energy converted by the wind generator depends solely on the rotor rotation frequency ω of the wind machine.

$$P_{\mathrm{wm}} = f(\omega_w) \tag{4}$$

The dynamic response equation of the synchronous machine SG is given below:

$$\Delta P_e(t) = -\frac{P_N T_{\mathrm{JS}}}{f_N}\frac{d\Delta f}{dt} \tag{5}$$

The inherent response of a synchronous generator (SG) shows no time delay. The kinetic energy stored in the rotating mass of the synchronous generator SG rotor is discharged instantaneously after identifying frequency deviations, thereby providing rapid network support during the initial stage of a disturbance. Virtual inertia control is added to simulate the dynamic response characteristics of SG. However, intrinsic communication and processing latencies within the power converter's feedback loop prevent an instantaneous response. The duration gap can be expressed analytically as a first-order inertial element.

$$\Delta P(s) = -\frac{1}{1 + sT_{\mathrm{w-s}}}\Delta P_0(s) \tag{6}$$

Introducing a first-order inertial term into the control mechanism results in a delayed response of the power delivery system from the hybrid wind-energy system after grid connection, thereby preventing a sudden change in auxiliary power. Nevertheless, the delayed termination of the auxiliary power may cause overspeed constraints to exceed the specified limit.

As shown in the simplified diagram in Figure 1, the frequency dynamics are interfered with by an abrupt variation of power, which is ΔP_{D0}. Determine whether the relevant WTGs are able to participate in frequency regulation, and resolve the frequency domain equations for the power system. The mathematical representation in the frequency domain for integrating wind-storage participation in frequency control is:

$$\Delta f(s) = \frac{\Delta P_{\mathrm{D0}}}{s}\left(\frac{1}{K_L + sT_{\mathrm{JS}} + \frac{K_G}{1+sT_G} + \frac{K_{\mathrm{WD}}+K_{\mathrm{BD}}+sK_{\mathrm{WI}}+sK_{\mathrm{BI}}}{1+sT_{\mathrm{w-s}}}}\right) \tag{7}$$

As shown in Figure 2, the fundamental frequency attributes mainly include the maximum rate of change of the frequency (Max-ROCOF), the peak frequency excursion ($\Delta f_{\max}$) and the final frequency offset ($\Delta f_{\rm ss}$). Through temporal domain evaluation of frequency behaviour, mathematical formulae of vital parameters are derived to determine the degree of impact of high-density wind power integration on dynamic frequency characteristics. The (Max-ROCOF) is marked immediately after the start of a disruption. Using the primary value property of the Laplace transform, this amount can be easily derived.

$$\begin{aligned}&\frac{d\Delta f(t)}{dt}\Big|_{t=0}=\lim_{s\to\infty}s^2\Delta f(s)\\&=\lim_{s\to\infty}s^2.\frac{\Delta P_{\rm D0}}{s}.\left(\frac{1}{K_{\rm L}+sT_{\rm JS}+\dfrac{K_{\rm G}}{1+sT_{\rm G}}+\dfrac{K_{\rm WD}+K_{\rm BD}+sK_{\rm WI}+sK_{\rm BI}}{1+sT_{\rm w\text{-}s}}}\right)\\&=\frac{\Delta P_{\rm D0}}{T_{\rm JS}}\end{aligned}\tag{8}$$

According to the temporal computational formula derived from Eq. 8 for the peak rate-of-change-of-frequency, the occurrence of a primary-order inertial lag significantly limits the capacity of simulated inertia regulation in wind turbines to mitigate the Max-ROCOF. It is affected by the primary electrical grid disturbance $\Delta P_{\rm D0}$ and the synchronous machine SG rotor inertia time constant $T_{\rm JS}$.

Oscillations of the electrical grid during irregular operation should remain within the specified functional range. The maximum variance of the peak frequency, $\Delta f_{\max}$, is influenced by factors such as the proportion of wind energy, ρ; the magnitude of energy disturbance, ΔP_d; total network inertia, H_g; synchronous generators operating conditions, etc. Regarding the temporal representation of frequency excursion, when time approaches infinity, the mathematical formula for the post-disturbance equilibrium frequency can be derived as follows:

$$\begin{aligned}&\frac{d\Delta f(t)}{dt}\Big|_{t=\infty}=\lim_{s\to 0}s^2\Delta f(s)\\&=\lim_{s\to 0}s^2.\frac{\Delta P_{\rm D0}}{s}.\left(\frac{1}{K_{\rm L}+sT_{\rm JS}+\dfrac{K_{\rm G}}{1+sT_{\rm G}}+\dfrac{K_{\rm WD}+K_{\rm BD}+sK_{\rm WI}+sK_{\rm BI}}{1+sT_{\rm w\text{-}s}}}\right)\\&=\frac{\Delta P_{\rm D0}\bullet s}{\dfrac{K_{\rm G}}{1+sT_{\rm G}}+\dfrac{K_{\rm WD}+K_{\rm BD}}{1+sT_{\rm w\text{-}s}}}\end{aligned}\tag{9}$$

Integrate Equation Eq. 8 with Eq. 9, it can be seen that with the increase of wind power integration, the total grid inertia decreases and the ROCOF increases. ROCOF is extremely high, it may trigger the under-frequency load shedding (UFLS) protection and thereby affect the stability of the entire power grid. Onshore wind parks cannot provide frequency regulation services or can only offer insufficient support, thus limiting their ability to assist the grid during power system disturbances, where the total system capacity is constant, and more synchronous generators are replaced by wind units, the maximum frequency deviation $\Delta f_{\max}$ will become increasingly severe; if a larger proportion of wind energy is integrated, it will significantly reduce the primary frequency modulation capacity of the power network, causing frequent trips due to high-frequency operation and low-frequency shedding of loads and other protection mechanisms.

B. ANALYSIS OF INERTIAL RESPONSE CHARACTERISTICS IN WIND-STORAGE SYSTEMS

In the electrical grid with high access to new energy sources, frequency stabilisation has become one of the primary difficulties. The transient frequency behaviour after grid disturbances is simultaneously affected by reserve margins, response speed, and the inherent regulation dynamics of variable power generators [16]. In light of the deficiencies in Reference [17], a synergistic primary frequency regulation approach combining wind power and energy storage has been proposed. Utilize the rotational kinetic energy of wind power generation units, make use of the flexibility of a hybrid energy storage system (HESS), thereby improving the stability of the power grid.

According to the regulating system of doubly-fed induction generator (DFIG), based on the available kinetic energy within this range, a dynamic weight-assignment scheme is proposed to achieve cooperative output effects by combining inertial-response control with droop-control mechanisms. In addition, a dynamic complementary-filtering frequency-partitioning approach is introduced to manage the HESS system at this stage. A unified approach to achieve intelligent energy allocation from the integrated wind-storage network in primary frequency regulation. Subsequent sections of this paper will examine the inertia and regulation potential of wind-storage integration from an energy perspective, as well as the energy distribution strategy throughout the architecture under various operating conditions.

1) Inertia Tuning of WTG

The inherent inertia time constant $H_{\rm sg}$ is based on the rotational kinetic energy of SG and is a fundamental mechanical attribute of traditional power units, and it may be regarded as a fixed parameter, and expressed as follows:

$$H_{\rm sg}=\frac{J_g\omega_e^2}{2S_N}\tag{10}$$

Wind turbine generators WTGs and power storage devices have potential energy reserves that can provide inertia support for the power system. In particular, these WTGs that use virtual inertia technology can manage the rotational kinetic energy of wind turbines to provide grid support after a system disturbance [18]. The kinetic energy $E_{\rm kw}$ stored in the rotating mass of a wind turbine generator (WTG) is a function of its moment of inertia and rotational speed:

$$E_{\rm kw}=\frac{1}{2}J_w\omega_r^2\tag{11}$$

Where $J_{\rm W}$ represents the physical mass moment of inertia of the rotor assembly and ω_r is the instantaneous rotational speed. Unlike synchronous generators, wind turbines are

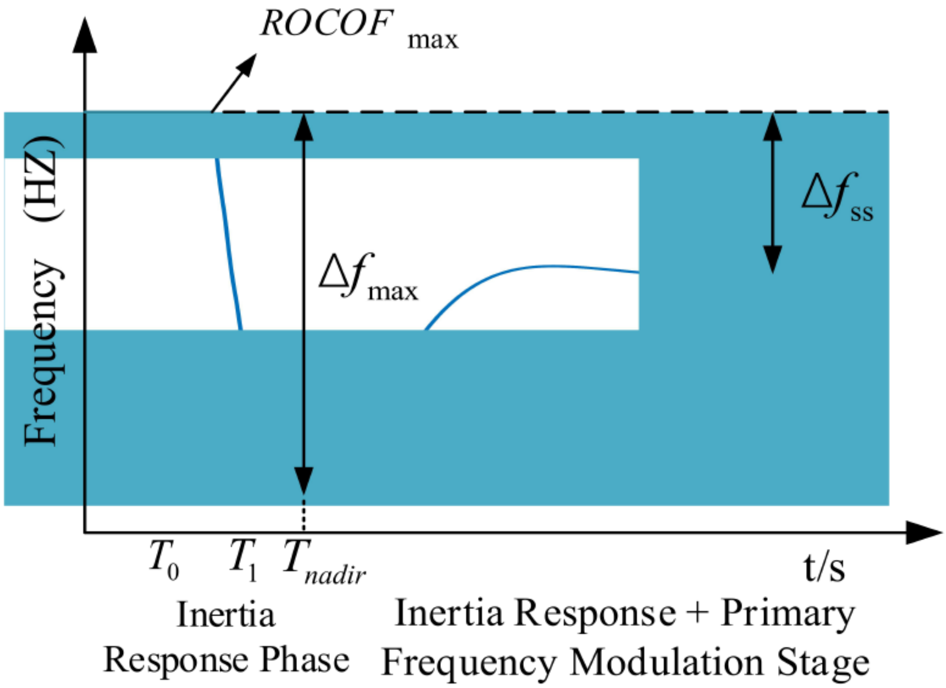

FIGURE 2. Fundamental Characteristics of Frequency Response

decoupled from the grid frequency. To emulate inertia, the virtual inertia time constant H_{vir} must be defined relative to the rated capacity S_{NW} and the nominal (rated) rotational speed $\omega_{n'}$, ensuring the definition remains a static machine attribute rather than a dynamic ratio. Equation (11) can be expressed as the fictitious mass of the wind power generator, J_{vw}, as follows:

$$J_{\mathrm{vw}} = \frac{J_w \omega_r d\omega_r}{\omega_e d\omega_e} = \frac{J_w \Delta\omega_r}{\Delta\omega_e} \frac{\omega_{r0}}{\omega_e} \tag{12}$$

Based on the characterisation of inertia time constants in synchronous generators, the equivalent virtual inertia time constant H_{vw} is thus defined as:

$$H_{\mathrm{vw}} = \frac{J_w \omega_n^2}{2S_{\mathrm{NW}}} \tag{13}$$

This constant represents the duration (in seconds) the WTG can provide its rated power solely from its stored kinetic energy while decelerating from rated speed to a standstill.

In actual operation at varying wind speeds, the available kinetic energy for frequency support is constrained by the operational speed range $[\omega_{r,\min}, \omega_{r,\max}]$. The starting rotor velocity ω_{r0} is affected by wind speed and defined as follows:

$$\omega_{r0} = \begin{cases} \dfrac{\lambda_{\mathrm{opt}} V}{R_t} & V_{\min} < V < V_{\max} \\ \omega_{\max} & V \geq V_{\max} \end{cases} \tag{14}$$

Where, λ_{opt} represents the optimal tip speed ratio of the rotor; V is the instantaneous wind speed at the generator; R_t is the length of the rotor blade; $V_{\min}$ is the minimum wind speed required for the turbine to enter its peak power regulation area; $V_{\max}$ is the maximum wind speed that the turbine can withstand; and $\omega_{\max}$ indicates the highest rotating speed that the unit can maintain continuously. Using Equations. (13) and (14), the simulated inertia time constant of the wind generator is calculated at various wind speeds and is shown as:

$$H_{\mathrm{vw}} = \begin{cases} \dfrac{\Delta\omega_r}{\Delta\omega_e} \dfrac{H_w}{\omega_e} \dfrac{\lambda_{\mathrm{opt}} V}{R_t} & V_{\min} < V < V_{\max}, \\ \dfrac{\Delta\omega_r}{\Delta\omega_e} \dfrac{H_w}{\omega_e} \omega_{\max} & V \geq V_{\max} \end{cases} \tag{15}$$

2) Energy Storage Battery Inertia Tuning

Unlike synchronous machines and wind power units, power storage devices are stationary devices. In terms of concept, storage facilities can be included in the active power regulation plan and use the power they have stored to provide simulated inertia to the power grid. However, to implement this strategy, a control-based emulation strategy is implemented via power electronic converters to provide virtual inertia support. Unlike physical mass, the virtual inertia of energy storage is defined by the converter's active power response characteristics. After a disturbance, the relationship between the battery's power output regulated by virtual inertia control and the equivalent kinetic energy support is expressed as:

$$\begin{aligned} W_B &= \int u_B i_B \, dt = u_B Q_N \gamma_{\text{soc}-0} = \int \frac{u_B i_B \, dt}{\omega_e d\omega_e} \omega_e d\omega_e \\ &= \int \frac{u_B Q_N d(1-\gamma_{\text{soc}})t}{\omega_e d\omega_e} \times \omega_e d\omega_e = \int J_{\text{vB}} \omega_e d\omega_e \end{aligned} \tag{16}$$

Where: γ_{soc} is the state of charge of the battery; Q_N is the nominal capacity of the battery; u_B and i_B are the battery's terminal voltage and current; the simulated inertia of the battery J_{vB} is given by:

$$J_{\text{vB}} = \frac{u_B Q_N d(1-\gamma_{\text{soc}})\gamma_{\text{soc}-0} J_g \omega_e}{\omega_e d\omega_e \, \gamma_{\text{soc}-0} J_g \omega_e} = -J_g \frac{\omega_e}{\gamma_{\text{soc}}} \frac{\Delta\gamma_{\text{soc}}}{\Delta\omega_e} \frac{W_B}{2E_g} \tag{17}$$

Where, E_g denotes the rotational kinetic energy that the equally rated synchronous generator has retained; $\gamma_{\text{soc}-0}$ represents the initial state of charge for that battery. According to the specific formulation of synchronous motor inertia time constants, it follows that the hypothetical inertia time constant for the battery can be represented as:

$$H_{\text{vB}} = \frac{J_{\text{vB}} \omega_e}{2S_{\text{NB}}} = -H_{\text{sg}} \frac{\omega_e}{\gamma_{\text{soc}}} \frac{\Delta\gamma_{\text{soc}}}{\Delta\omega_e} \frac{W_B}{2E_g} \tag{18}$$

C. ENERGY STORAGE CAPACITY ALLOCATION IN WIND-STORAGE COMBINED FREQUENCY REGULATION

To reduce the electrical energy consumption in the frequency stabilisation stage, a velocity monitoring strategy with velocity buffers is adopted for the wind generator, and differential momentum management with rapid disconnect functions is implemented on the power storage system. The architecture of the wind-storage integrated regulation system shown in Figure 3. Includes wind, storage pseudo-inertia regulation, FM signal production and controller coefficient optimisation components. In the wind-storage virtual inertia regulation module, control inhibition is realised at the end of the inertia response, and a first-order inertia element is added to the wind-storage active regulation loop for smooth switching of windstorage inertia management.

The scale of energy storage is a key element that determines whether a hybrid wind-storage facility can be integrated into the grid for frequency regulation; this research explores wind-induced frequency drops, and the capacity distribution of storage units participating in electrical system frequency regulation is an essential engineering parameter. As wind speeds continue to increase, the storage capacity required by wind farms also increases; then use the peak power of wind farms to meet the park's energy storage needs in terms of both power and capacity at all wind speeds.

1) Coordinated Allocation of Frequency Regulation Power Among Wind Turbines in Wind Farms

Based on the primary indicators of system frequency stability [19]. The frequency shift velocity (df/dt) and frequency fluctuation ($\Delta f_{\max}$) are taken as key indicators to evaluate the inertia requirement of the new energy FM in this study. Based on the operational requirements of the target grid and considering the thresholds for Under-Frequency Load Shedding (UFLS), this work sets the frequency shift rate at 0.5 Hz/s, the maximum allowable transient frequency excursion $\Delta f_{\max}$ at 0.8 Hz (ensuring $f > 49.2$ Hz), and the static frequency deviation Δf_{ss} at 0.2 Hz to provide a conservative safety margin for storage sizing. Assuming that the wind farm (with capacity P_n MW) can provide an equivalent inertial response H_{VW} to traditional power generation units, the turbine outputs P_{wh} and needs to be equipped with a storage volume of E_{wh} to meet the special frequency regulation limit.

$$P_{\text{wh}} = P_n \cdot 2H_{\text{vw}} \frac{df}{dt} \tag{19}$$

$$E_{\text{wh}} = P_n H_{\text{vw}} \left(f_0^2 - f_{\min}^2\right) \tag{20}$$

Where: H_{VW} is the inertia coefficient corresponding to the nominal wind speed, defined as 4 s; the peak frequency variation rate $df/dt_{\max}$ is set at 0.5 Hz/s (considered as 0.01/s); The lowest frequency $f_{\min}$ is 0.96 ($f_{\min} = 48$ Hz), and the required power $P_{\text{wh}} = 8\% P_n$ (MW), with the storage energy $E_{\text{wh}} = 0.087 P_n$ (kWh). The main FM power and capability for capacity to be supplied by the wind facility once it has primary frequency control capacity are:

$$P_{\text{wp}} = -P_n K_{\text{WD}} \Delta f \tag{21}$$

$$E_{\text{wp}} = P_p T_d \tag{22}$$

a: 1) Safety constraints on fan rotor speed.

If the perturbed power ΔP_{D0} is greater than zero, the fan needs to release its accumulated mechanical energy to make up for the insufficient power, so that the rotor speed ω_r will decrease; otherwise, if ΔP_{D0} is less than zero, the fan will take in kinetic energy and increase the speed ω_r. The fan velocity restriction is expressed as follows:

$$\Delta\omega_{\max} = \begin{cases} \omega_{r0} - \omega_{r\min} & \Delta P_d > 0 \\ \omega_{r\max} - \omega_{r0} & \Delta P_d < 0 \end{cases} \tag{23}$$

Where: $\Delta\omega_{\max}$ represents the peak variation magnitude of fan velocity in the speed security limit; $\Delta\omega_{r0}$ represents the initial rotating speed of the impeller; $\omega_{r\max}$ is the upper bound speed of the rotor during secure operation; $\omega_{r\min}$ is the lower limit speed of the rotor during secure operation. Taking a 2 MW Wind Turbine Generator (WTG) as an example, set $H_W = 4$ s, $K_{\text{opt}} = 1/(1.23)$, $\omega_{r\max} = 1.2$ pu, $\omega_{r\min} = 0.8$ pu.

$$\Delta E_K = \begin{cases} \frac{1}{2} J \left(\omega_{r0}^2 - \omega_{r\min}^2\right) & \Delta P_d > 0 \\ \frac{1}{2} J \left(\omega_{r\max}^2 - \omega_{r0}^2\right) & \Delta P_d < 0 \end{cases} \tag{24}$$

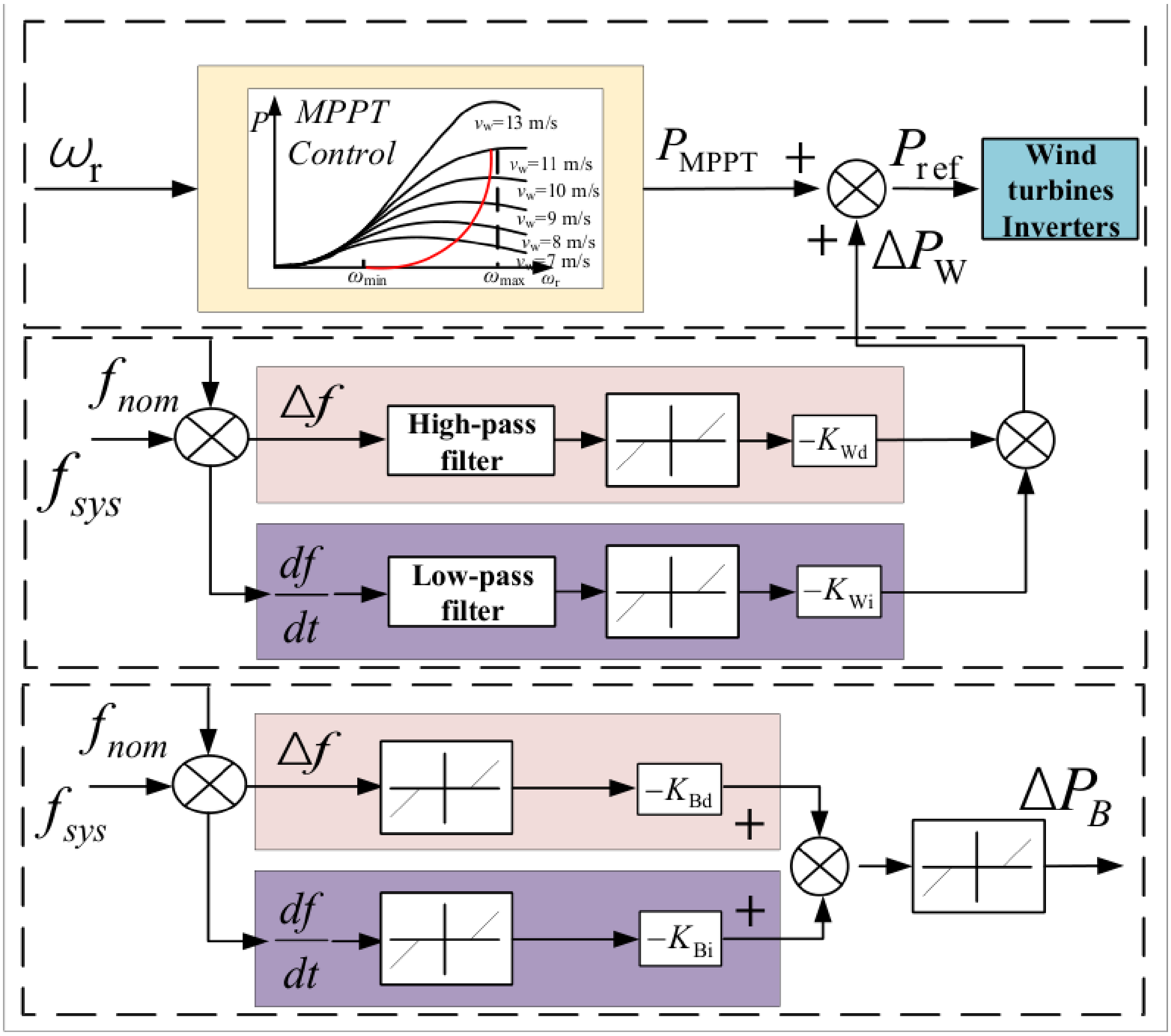

FIGURE 3. Wind-Storage Combined Frequency Regulation Control Block Diagram

Based on the equation Eq. Based on equation (24), the mathematical formula for the change in rotor energy within the safety range of wind speed is derived.

$$E_{\mathrm{wh}} = \frac{\Delta E_K}{E_{\mathrm{Kn}}} = \begin{cases} \dfrac{\omega_{r0}^2 - \omega_{r\,\mathrm{min}}^2}{\omega_n^2} & \Delta P_d > 0 \\ \dfrac{\omega_{r\,\mathrm{max}}^2 - \omega_{r0}^2}{\omega_n^2} & \Delta P_d < 0 \end{cases} \tag{25}$$

b: 2) Turbine output power constraints.

To ensure the safety of the turbine function, limiting the output power within a specified range is necessary. The power of the fan is given by:

$$P_{\mathrm{ew}} = \begin{cases} K_{\mathrm{opt}} \times \omega_{\mathrm{r0}}^3 & \omega_{\mathrm{rmin}} < \omega_{\mathrm{r}} < \omega_{\mathrm{rmax}} \\ P_{\mathrm{n}} & \omega_{\mathrm{r}} > \omega_{\mathrm{rmax}} \end{cases} \tag{26}$$

Where: P_{ew} is the rotor electromagnetic power, K_{opt} is the peak power tracking proportion factor, $\omega_{r\,\mathrm{min}}$ is the minimum rotor velocity in the power tracking area, and P_n is the rated power of the wind turbine. Based on Equation Eq. (26) under the power limit, the active power assistance boundary of the wind generator can be defined as:

$$\Delta P_{\mathrm{max}} = \begin{cases} K_{\mathrm{opt}}\omega_{\mathrm{n}}^3 - K_{\mathrm{opt}}\omega_{\mathrm{r0}}^3 & \Delta P_{\mathrm{d}} > 0 \\ K_{\mathrm{opt}}\omega_{\mathrm{r0}}^3 - K_{\mathrm{opt}}\omega_{\mathrm{min}}^3 & \Delta P_{\mathrm{d}} < 0 \end{cases} \tag{27}$$

According to (27), the mathematical expression for the power-augmenting threshold of the wind generator is derived.

$$P_{\mathrm{wh}} = \begin{cases} \dfrac{K_{\mathrm{opt}}\omega_{\mathrm{n}}^3 - K_{\mathrm{opt}}\omega_{\mathrm{r0}}^3}{K_{opt}\omega_{\mathrm{n}}^3} & \Delta P_{\mathrm{d}} > 0 \\ \dfrac{K_{\mathrm{opt}}\omega_{\mathrm{r0}}^3 - K_{\mathrm{opt}}\omega_{\mathrm{min}}^3}{K_{\mathrm{opt}}\omega_{\mathrm{n}}^3} & \Delta P_{\mathrm{d}} < 0 \end{cases} \tag{28}$$

2) Capacity Allocation for Wind-Storage Combined Frequency Regulation under Low Wind Speeds

Wind power generation equipment, equipped with additional rules, may also have a frequency regulation capability similar to SG; however, the speed of its rotating part is determined by local weather conditions; therefore, the inertia and supporting effects brought by the wind turbine to external forces change significantly under different strengths of wind, thereby affecting its speed. Take $\Delta P_{\mathrm{D0}} > 0$ as an example, the frequency rate of change is set to 0.5 Hz/s, $df/dt_{\max} = 0.5$ Hz/s, $\Delta f_{\max} = 2$ Hz, and the steady-state frequency deviation $\Delta f_{\mathrm{ss}} = 0.2$ Hz for example. When the rotor speed $\omega r0$ approaches the lower operational limit $\omega r\min$ (e.g., 0.8 pu), the wind turbine exits the frequency regulation mode to avoid the risk of stalling or aerodynamic instability.In this state, the virtual inertia control loop is physically decoupled, and the system transition logic explicitly dictates that 100% of the required frequency response power and energy capacity shall be autonomously provided by the energy storage system:

$$P_{\mathrm{B}-1} = P_{\mathrm{wh}} + P_{\mathrm{wp}} \tag{29}$$

$$E_{\mathrm{B}-1} = E_{\mathrm{wh}} + E_{\mathrm{wp}} \tag{30}$$

It is known from equations 8 and 9:

$$\Delta P_{\mathrm{D01}} = \frac{df}{dt}_{\max} T_{\mathrm{JS}} \tag{31}$$

$$\Delta P_{\mathrm{D02}} = \frac{\Delta f_{\mathrm{ss}}}{\frac{K_G}{1+sT_G} s} \tag{32}$$

$$\Delta P_{\mathrm{D03}} = F[\Delta f_{\max}, H_{\mathrm{sg}}] \tag{33}$$

To meet the frequency limitations simultaneously, when the disturbance amplitude exceeds any of the reference values, the collaborative management strategy is activated for that window. If $\Delta P_{\mathrm{D0}} > \min[\Delta P_{\mathrm{D01}}, \Delta P_{\mathrm{D02}}, \Delta P_{\mathrm{D03}}]$, then both the synchronous motor and the storage unit need to operate in conjunction to satisfy the frequency regulation requirement.

3) Frequency Regulation Capacity Allocation for Wind-Storage Hybrid Systems at Rated Wind Speed

When the rotor speed ω_{r0} of the wind turbine reaches $\omega_r = 1.0$ pu, the wind park has FM function, and its FM power and FM capacity required by the facility should be adjusted in response to the size of the disturbance, the grid operation condition and the frequency security index.

The wind turbine provides inertial support power $P_{\mathrm{wh}} = 8\% P_n$ and capacity $E_{\mathrm{wh}} = 0.087P_n$ (kWh), and provides primary FM power $P_{\mathrm{wp}} = 10\% P_n$ (MW) and capacity $E_{\mathrm{wp}} = 0.83P_n$ (kWh). The power under the speed safety constraint and power constraint is $P_{h2} = 0.42P_n$ (MW) and demand capacity $E_{h2} = 0.25P_n$ (kWh). It is evident that the required auxiliary strength and support capability to ensure the grid frequency stability vital metric have exceeded the electrical output and resource levels that the wind machine can produce within the safety limit of the wind turbine rotation speed and power limitation.

$$\Delta P_{\mathrm{D0a}} = \frac{df}{dt}_{\max} (T_{\mathrm{JS}} + T_w) \tag{34}$$

$$\Delta P_{\mathrm{D0b}} = \frac{\Delta f_{\mathrm{ss}}}{\left(\frac{K_G}{1+sT_G} + \frac{K_{\mathrm{WD}}}{1+sT_D}\right) s} \tag{35}$$

$$\Delta P_{\mathrm{D0c}} = F[\Delta f_{\max}, H_{\mathrm{sg}} + H_{\mathrm{vw}}] \tag{36}$$

If the turbine can provide frequency support, if

$$\min[\Delta P_{\mathrm{D01}}, \Delta P_{\mathrm{D02}}, \Delta P_{\mathrm{D03}}] < \Delta P_{\mathrm{D0}} < \min[\Delta P_{\mathrm{D0a}}, \Delta P_{\mathrm{D0b}}, \Delta P_{\mathrm{D0c}}],$$

the synchronous generator and the turbine need to be operated at the same time to meet the frequency stabilisation requirement. If

$$\Delta P_{\mathrm{D0}} > \min[\Delta P_{\mathrm{D0a}}, \Delta P_{\mathrm{D0b}}, \Delta P_{\mathrm{D0c}}],$$

the synchronous generator and the wind turbine need to work simultaneously and be equipped with energy storage to meet the frequency stability demand.

III. ENERGY STORAGE PARAMETER SETTINGS CONSIDERING FREQUENCY SAFETY CHARACTERISTICS

Generally, a brief frequency drop during the initialisation of power storage is acceptable; subsequently, as the system's own stability mechanism recovers from oscillation. However, it is still necessary to predict the following frequency path after activation and simultaneously limit the length of this dip as well as its minimum frequency level. When power storage is included, the frequency pattern will no longer be a response to a single disturbance but also require the oscillation behaviour brought about by the storage of energy for power generation. The derivative of frequency deviation in a grid that includes wind power generation and energy storage is defined as follows:

$$\Delta f \left.\frac{df}{dt}\right|_{\mathrm{t=0}} \frac{P_{\mathrm{D0}}}{2H_{\mathrm{sys}}} \frac{P_{\mathrm{D0}}}{2(H_{\mathrm{sg}} + H_{\mathrm{vB}} + H_{\mathrm{vw}})}_{\mathrm{rocof-max}} \tag{37}$$

Based on the relevant frequency stability limits, the inherent requirement for the grid in a specific security buffer is initially determined. Based on the power demand that power storage devices need to provide, the corresponding storage quantity will then be allocated. The dynamic response provided by the batteries is related to their magnitude in the following manner:

$$H_{\mathrm{vB}} = \frac{J_{\mathrm{vB}}\omega_e}{2S_{\mathrm{NB}}} = -H_{\mathrm{g1}} \frac{\omega_e}{\gamma_{\mathrm{soc}}} \frac{\Delta\gamma_{\mathrm{soc}}}{\Delta\omega_e} \frac{E_{\mathrm{B}-2}}{2E_g} \tag{38}$$

In full application of the system's inherent frequency self-balancing function, a short-term oscillation with an upper limit deviation can be permitted right after the energy storage device is activated. Therefore, when using the energy storage device requires trigger conditions in different situations, resulting in varying amounts of frequency offset. The connection among system frequency, the delivered power of the energy storage device, and duration is described by the following formula: The minimum frequency value after the energy storage intervention serves as the basis for selecting frequency regulation. The smaller this minimum frequency value, the greater the risk to the stability of the power grid frequency. As a result, it is necessary to specify the frequency spectrum after the intervention for the minimum value:

$$F(t) = \frac{P_{\mathrm{D0}}}{2(H_{\mathrm{sg}} + H_{\mathrm{vB}} + H_{\mathrm{vw}})} F(t_0) + \frac{P_{\mathrm{B-2}}}{2(H_{\mathrm{sg}} + H_{\mathrm{vB}} + H_{\mathrm{vw}})} F(t_B) \tag{39}$$

Differentiating Equation 39 provides the necessary basis for analysing the system frequency's nadir. Taking into account the relevant security limitations, the power-generating capability of the energy-storage apparatus shall therefore be adjusted accordingly. The block diagram of the adaptive energy storage mechanism is shown in Figure 4. Initially, the entire expression for $\Delta f(t)$ is derived. Subsequently, temporal difference operations are carried out according to the formula above. If it is expected that the frequency will continue to be above the threshold, there is no need for energy storage participation. If the frequency is predicted to fall below the set threshold, then based on the energy storage attributes, $P_{\mathrm{B-2}}$, $E_{\mathrm{B-2}}$, and t_B will be activated. Finally, through frequency response attributes and taking into account the system's inherent frequency stabilisation capacity plus related wind environment constraints, perform energy storage scheduling.

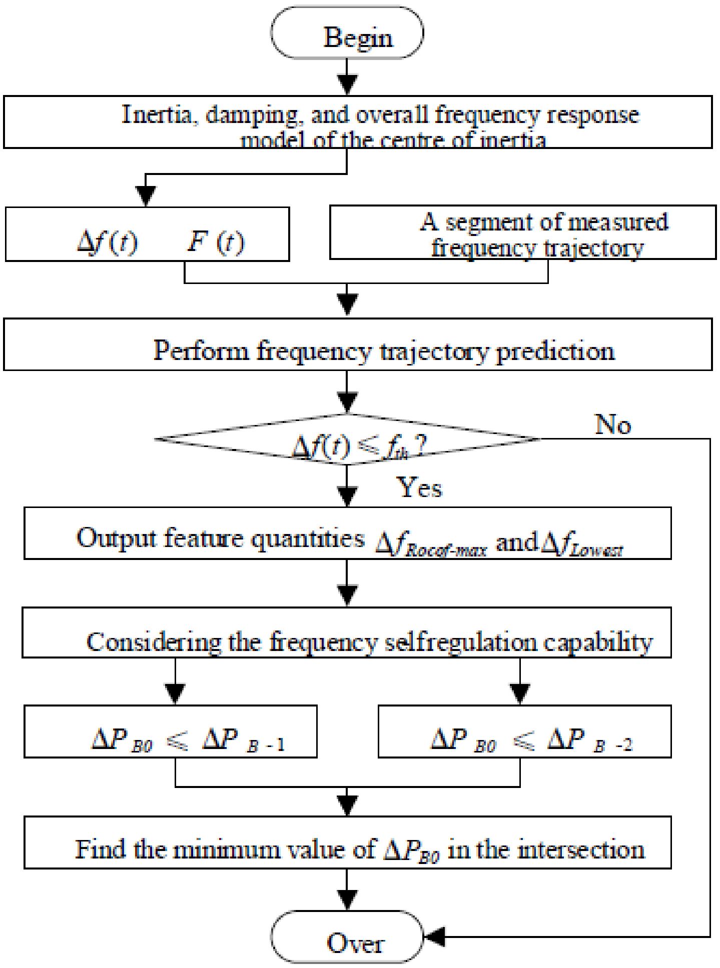

FIGURE 4. Algorithm Flowchart

As shown in Figure 5, the necessary FM power and FM capacity for the wind farm are provided by the energy storage system; this requires the integration of the wind farm's control strategy, including whether to install energy storage and subsequent detailed design.

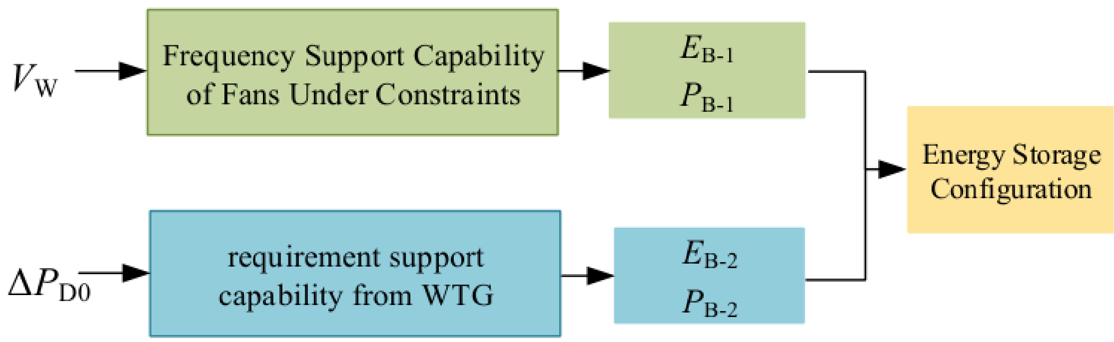

FIGURE 5. Energy Storage Configuration Flowchart

IV. CASE STUDY ANALYSIS

Based on the above assessment, this part will examine the effectiveness of the proposed wind-storage integrated frequency-quick adjustment management scheme through a refined IEEE 3-unit 9-node system in Digsilent PowerFactory software.

As shown in Figure 6, the improved IEEE 3-machine 9-node system consists of three electrical generating units plus an energy storage system, which includes a hydroelectric unit G1 equipped with an IEEE G3-type speed governor, a steam turbine unit G2 installed with an IEEE G1-mode speed controller, and a wind turbine unit G3 featuring virtual inertia management. The energy storage facility is uniformly arranged close to the outlet of the wind farm and connected to the power grid via power electronic devices. The selected storage type is a power-based storage System, such as Supercapacitors, that can meet the demand for operation at a wind farm by utilising its fast-response attribute and High Power-to-energy ratio for frequency modulation. G1 serves as the main reference generator specifically. To verify the accuracy of the frequency response model simulation results, the analytical system parameters are set out in Table 1.

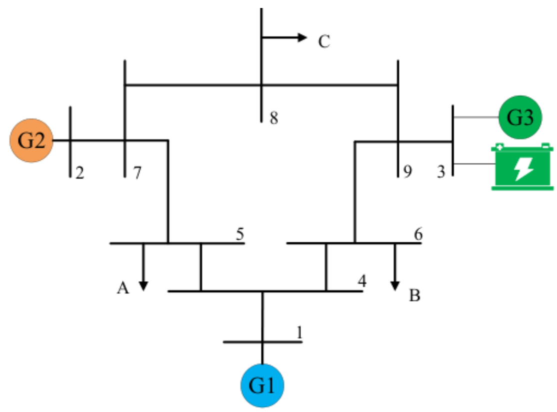

FIGURE 6. IEEE-3-machine 9-node Simulation Architecture Diagram

TABLE 1. Improved IEEE 3-machine 9-node system generator parameters

Generator type	Number	S_N/MVA	H/s
Hydraulic turbine	G1	247.5	9.551 516
Steam turbine	G2	200.0	5.333 333
Wind farm	G3	120.0	4

A. ANALYSIS OF FREQUENCY CHARACTERISTICS IN COMBINED WIND-STORAGE FREQUENCY REGULATION UNDER LOW WIND SPEEDS

Considering the situation where $\Delta P_{D0} > 0$, based on [20] for fan variables. In a low-wind situation, the wind generator runs at its minimum rotation speed and does not have frequency modulation capability; at this time, energy storage provides the regulation energy required for the wind park. The output capacity of the wind farm is 20% of the maximum wind power (P_W). A numerical simulation study is conducted to explore the dynamic frequency response under the operation mode of wind-storage integrated frequency regulation.

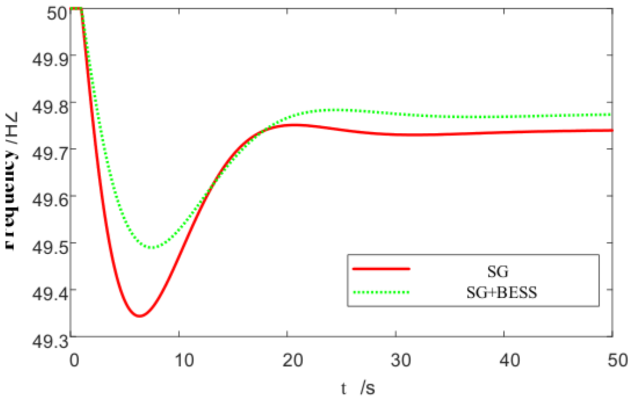

FIGURE 7. Energy storage participating exclusively in grid frequency regulation during light interference

Scenario 1 (frequency regulation by synchronous machines alone): A 20 MW fluctuating load, with a frequency slope of 0.5 Hz/s, $df/dt_{\max} = 0.5$ Hz/s, peak deviation $\Delta f_{\max} = 2$ Hz, and a steady-state frequency shift $\Delta f_{ss} = 0.5$ Hz. According to Equations 8 and 9, the minimum inertia necessity H_{smin} of this system is 2.8 seconds; the droop parameter K_{WD} is set to 25. With the implementation of wind-storage integrated management, the inertia provided by the synchronous machine is 5.3 s; therefore, additional inertia management is not required for the wind and storage units.

Scenario 2 (wind turbines join frequency stabilisation provided by power storage): A sudden increase in demand of 40 MW results in a minimum inertia requirement H_{smin} of 4.8 seconds, approaching the inertia limit that the synchronous generator can offer. The grid sends a power-adjustment instruction. Wind power generation units need to have frequency modulation capabilities. Using frequency modulation instructions and simulation variables to derive the system's inertial response factors. Wind power units operate at very low rotational speeds, lack frequency modulation capabilities, and therefore require a storage facility that can provide active frequency regulation capacity to work in conjunction with a synchronous motor and wind generators to achieve system inertia support and droop regulation. The energy storage system's power (14 MW) and capacity (28.8 MWh) are specified. Illustrations 7 and 8 show the frequency distribution pattern under different disturbances, and when wind power generators do not participate in active frequency modulation in low wind speed conditions, Tables 2 and 3 are used to evaluate the frequency response property.

The frequency response characteristics of the system under different power disturbances indicate that when the disturbance power is 20 MW, under conditions where the wind-storage system is not participating in frequency regulation, the lowest frequency point is 49.3442 Hz, the rate of change of frequency ROCOF is -0.2258 Hz/s (<0.5 Hz/s limit), and the final deviation is 49.7393 Hz, meeting the system frequency safety criteria requirements. However, when the disturbance increases to 40 MW, the system's inherent frequency regulation capability becomes insufficient: without energy storage frequency regulation, the lowest frequency point drops sharply to 48.6858 Hz (triggering the risk of lowfrequency load shedding), the ROCOF deteriorates to -0.4517 Hz/s, and the steady-state frequency deviation expands to 49.4613 Hz, severely deviating from the safe operating range. Upon engaging the configured energy storage system (10 MW/23.6 MWh) for frequency regulation, key frequency metrics significantly improved: the lowest frequency point increased to 48.9415 Hz (an improvement of 0.256 Hz compared to the no-energy-storage scenario), ROCOF optimised to -0.3168 Hz/s (a reduction of 29.9%), and steady-state deviation narrowed to 49.5324 Hz. The results demonstrate that the system possesses autonomous frequency stability capabilities under small disturbances; in large disturbance scenarios, energy storage effectively suppresses the rate of frequency decline ROCOF and the depth of frequency drop (Δf_{ss}) by rapidly providing active grid support, making it a critical measure for ensuring transient frequency safety in high wind power penetration systems.

TABLE 2. Frequency Characteristics

$\Delta P_{\text{D0}} = 20$ MW	ROCOF/ ($\text{Hz}\cdot\text{s}^{-1}$)	f_{nadir}/ Hz	f_{ss}/ Hz
Wind-storage without FM	-0.2258	49.3442	49.7393
Energy storage with FM	-0.1527	49.4899	49.7732

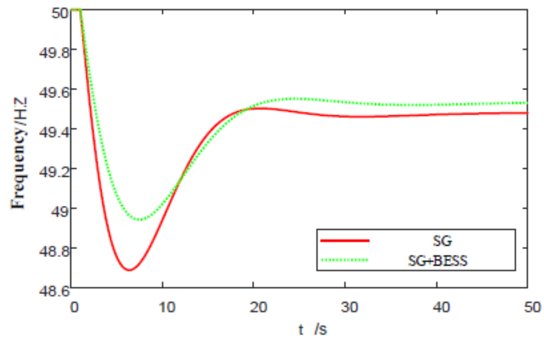

FIGURE 8. Battery Storage only participates in grid frequency regulation under slight disturbances

TABLE 3. Frequency Characteristics

$\Delta P_{\text{D0}} = 40$ MW	ROCOF/ ($\text{Hz}\cdot\text{s}^{-1}$)	f_{nadir}/ Hz	f_{ss}/ Hz
Wind-storage without FM	-0.4517	48.6858	49.4613
Energy storage with FM	-0.3168	48.9415	49.5324

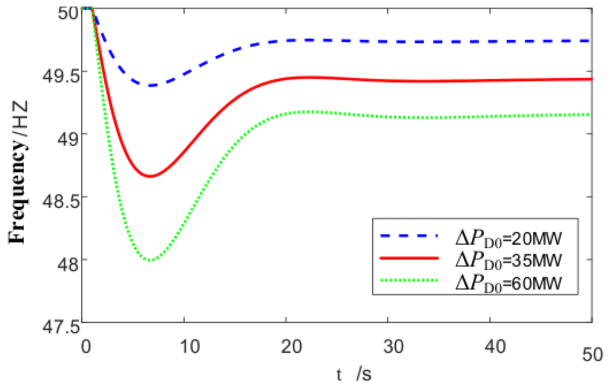

FIGURE 9. Time-domain Simulation Plots under Different ΔP_{D0} Conditions

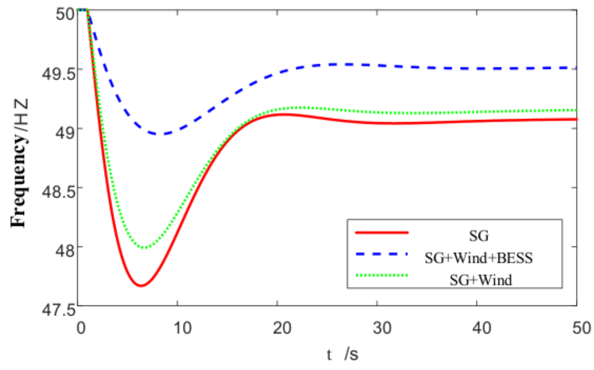

FIGURE 10. Time-domain Simulation Plots under Different ΔP_{D0} Conditions

TABLE 4. Frequency Characteristics under Different ΔP_{D0}

ΔP_{D0}	ROCOF/ (Hz·s^{-1})	f_{nadir}/ Hz	f_{ss}/ Hz
20	-0.2062	49.3864	49.7409
35	-0.3494	48.7226	49.4403
60	-0.4723	48.0193	49.1985

B. ANALYSIS OF FREQUENCY CHARACTERISTICS FOR COMBINED WIND-STORAGE FREQUENCY REGULATION AT RATED WIND SPEED

At a rated wind velocity and under frequency modulation, as shown in Figure 9, the frequency response curves for different perturbation sizes are presented. Table 4 shows the main indicators of various disturbances. Simulated evaluation of system oscillation properties in three scenarios: wind generation excluding frequency control, wind generation integrating frequency control, and wind-storage synergy for frequency control, as shown in Figure 10. Oscillation quality metrics are presented in Table 5 with a contrast.

As shown in Figure 9, under a 20 MW disturbance, the system can maintain good frequency characteristics. Under a 35 MW disturbance, $\Delta f_{max} < 2$ Hz meets the requirements, but $\Delta f_{ss} > 0.5$ Hz, and the steady-state frequency deviation exceeds the frequency response criteria. Under a 60 MW disturbance, both Δf_{max} and Δf_{ss} fail to meet the requirements. As the disturbance increases to 60 MW, the participation of wind turbines and synchronous generators in frequency regulation can no longer meet the system's frequency characteristic requirements, and the setting of energy storage power becomes a critical condition for maintaining system frequency compliance. When a 60 MW disturbance occurs, each site will adopt different frequency modulation strategies to restore system frequency after the disturbance. The above situations are referred to as:

Scenario 1 (synchronous generator alone supports frequency):

Scenario 2 (wind turbine participates in frequency support):

Scenario 3 (wind turbine and energy storage joint frequency regulation):

TABLE 5. Frequency Response under Large Disturbances

$\Delta P_{D0} = 40$ MW	ROCOF/ (Hz·s^{-1})	f_{nadir}/ Hz	f_{ss}/ Hz
Wind-storage without FM	-0.6037	47.6758	49.0749
Individual wind with FM	-0.4723	48.0193	49.1985
Wind-storage with FM	-0.2840	48.9517	49.5107

As shown in Figure 10 and Table 5, under the condition of rated wind speed and active frequency modulation, wind energy can provide both kinetic response and backup support to maintain the stability of the grid frequency.

The ROCOF magnitude of the frequency variation under the integrated wind-storage frequency control approach is –0.2840 Hz/s, which is a 39.9% decrease from wind-only modulation (–0.4723 Hz/s). Based on this result, it can be known that power storage is more effective in supplying a quick virtual inertia assist. The integrated wind-storage combination system for frequency regulation has raised the lower limit of the frequency standard above the safe margin zone (48.9517 Hz) and avoided the situation of under-frequency load shedding (UFLS). The steady-state deviation of the hybrid wind-storage configuration (49.5107 Hz) is significantly better than that of isolated wind turbine frequency regulation (49.1985 Hz). As a result, during the disruption of the system's normal operation, an increase in the minimum frequency level occurred, a decrease in steady-state frequency deviation appeared, and its behaviour met the requirements for grid frequency stability. The wind-storage hybrid frequency control utilised the energy storage system's fast response to reduce the rate of change in the system's frequency, increase the lower limit of the system's frequency, and enhance the transient-frequency robustness of the system.

V. CONCLUSION

In the context of the ongoing deepening of the ‘double high’ trend, the power system is facing a weakening of inertial support and a decline in interference resistance, which is exacerbating the severity of frequency stability issues and limiting the further large-scale development of carbon-free energy sources such as wind power. Therefore, the active participation of wind power generation in system frequency regulation has become an inevitable trend in the construction of a new power system. The present work focuses on the application of (DFIG) in frequency regulation, with the main work covering the following aspects:

1. Clarifying the underlying mechanisms: Based on the SFR model, this study quantitatively reveals the key mechanisms by which high wind power penetration reduces system inertia and deteriorates frequency dynamics (ROCOF, $\Delta f_{\max}$, and Δf_{ss}).

2. Analysing frequency regulation strategies: We compared and contrasted the main frequency regulation technologies of DFIG (virtual inertia, load shedding, energy storage assistance, and coordination), explaining their principles, performance, and limitations.

3. Proposed wind-storage configuration method: We innovatively proposed a layered configuration method for wind-storage joint frequency regulation energy storage capacity that considers wind speed conditions, frequency safety indicators, and wind turbine constraints (speed safety, power limits), providing quantitative basis for engineering applications.

4. Verification of Control Performance: Simulation results show that: at low wind speeds, energy storage effectively improves frequency response; at rated wind speeds, wind-storage joint control significantly outperforms single-turbine frequency regulation, significantly reducing ROCOF, improving the lowest frequency point, reducing steady-state deviation, and successfully addressing the issue of secondary frequency drops caused by speed recovery after frequency regulation.

ABBREVIATIONS

The following abbreviations are used in this manuscript:

ROCOF	Rate of Change of Frequency
WTG	Wind Turbine Generator
DFIG	Doubly Fed Induction Generator
HESS	Hybrid Energy Storage System
LV	Low-Voltage
BESS	Battery Energy Storage System
SCESS	Super Capacitor Energy Storage Sy
RSC	Rotor Speed Control
PAC	Pitch Angle Control
PMU	Phasor Measurement Unit
WF	Wind Farm
FM	Frequency Modulation
SG	Synchronous Generator
MPPT	Maximum Power Point Tracking

AUTHOR CONTRIBUTIONS

Jian Zhang designed, collected and analyzed the data, and drafted the manuscript. Jian Zhang conducted the study, critically revised the manuscript for important intellectual content, and gave final approval of the version to be published.

Jian Zhang participated fully in the work, take public responsibility for appropriate portions of the content, and agreed to be accountable for all aspects of the work in ensuring that questions related to the accuracy or integrity of any part of the work are appropriately investigated and resolved.

CONFLICTS OF INTEREST

The authors declare no conflict of interest.

FUNDING

This research received no external funding.

ACKNOWLEDGEMENTS

Not applicable.

REFERENCES

[1] J. C. Smith and C. Clark, “Tomorrow’s Power Supply: The Path to Synthesis,” IEEE Power Energy Mag., vol. 17, pp. 19–23, 2019, doi: 10.1109/MPE.2019.2933283.

[2] H. Bevrani, A. Ghosh, and G. Ledwich, “Integration of solar and wind power: Overview and new approaches to frequency regulation,” IET Renew. Power Gener., vol. 4, pp. 438–457, 2010, doi: 10.1049/iet-rpg.2009.0049.

[3] M. F. M. Arani and Y. A. R. I. Mohamed, “Dynamic droop control for wind turbines participating in primary frequency regulation of microgrids,” IEEE Trans. Smart Grid, vol. 9, pp. 5742–5751, 2017, doi: 10.1109/TSG.2017.2696339.

[4] C. Chen, Y. Su, and T. Yang, “Virtual inertia simulation control technique for DFIG-based wind farms to enhance network frequency regulation performance,” Electr. Power Syst. Res., vol. 216, 109076, 2023, doi: 10.1016/j.epsr.2022.109076.

[5] M. Sun, Y. Min, and L. Chen, “Performance optimisation for auxiliary frequency regulation of wind turbine units and integration with synchronous motors,” CSEE J. Power Energy Syst., vol. 7, pp. 78–85, 2020, doi: 10.17775/CSEEJPES.2020.00860.

[6] X. Lyu, Y. Jia, and Z. Dong, “Adaptive frequency responsive regulation of wind farms considering wake interactions,” J. Mod. Power Syst. Clean Energy, vol. 9, pp. 1066–1075, 2021, doi: 10.35833/MPCE.2020.000237.

[7] M. Sun, Y. Sun, and L. Chen, “A new temporary frequency regulation strategy for wind turbine generators focusing on synchronous generator coordination,” IEEE Trans. Sustain. Energy, vol. 13, pp. 1011–1020, 2022, doi: 10.1109/TSTE.2022.3142914.

[8] M. V. Kazemi, S. J. Sadati, and S. A. Gholamian, “Adaptive frequency regulation of microgrids based on fractional-order control and stability-enhanced data-driven methods,” IEEE Trans. Smart Grid, vol. 13, no. 4, pp. 381–392, 2021, doi: 10.1109/TSG.2021.3109627.

[9] C. Zhao, D. Sun, X. Zhang, et al., “A dual-phase power allocation mechanism for multiple wind farms participating in primary frequency regulation,” IEEE Trans. Power Syst., vol. 38, pp. 5009–5021, 2022, doi: 10.1109/TPWRS.2022.3224971.

[10] G. Tu, Y. Li, and J. Xiang, “Joint regulation of wind turbine rotor velocity and blade pitch for precise and efficient frequency response in power systems,” IEEE Trans. Power Syst., vol. 37, no. 20, pp. 3566–3576, 2021, doi: 10.1109/TPWRS.2021.3136822.

[11] Y. Wang, D. Wang, and Y. Tang, “A grouped integrated wind-forecasting framework based on ARMA, PSO-SVM and partitioning techniques,” IEEE Access, vol. 8, pp. 17071–17079, 2020, doi: 10.1109/ACCESS.2020.2968390.

[12] X. Tian, W. Wang, Y. Chi, et al., "Virtual inertia control optimisation of DFIG and equivalent inertia time constant evaluation for power grid," IET Renew. Power Gener., vol. 12, pp. 1733–1740, 2018, doi: 10.1049/iet-rpg.2018.5063.
[13] P. M. Anderson and M. Mirheydar, "Simplified system frequency response model," IEEE Trans. Power Syst., vol. 5, pp. 720–729, 1990, doi: 10.1109/59.65898.
[14] Y. Ren, C. Wan, R. Xiao, et al., "A unified frequency response characterisation framework for wind-dominated grids," in Proc. 2023 IEEE/IAS Ind. Commercial Power Syst. Asia (I&CPS Asia), Shanghai, China, 2023, pp. 422–428, doi: 10.1109/ICPSAsia58343.2023.10294519.
[15] L. Liu, W. Li, B. Ba, et al., "A mathematical framework for frequency minimum estimation after a substantial disturbance," IEEE Trans. Power Syst., vol. 35, pp. 2527–2536, 2020, doi: 10.1109/TPWRS.2019.2963706.
[16] Y. Jia, N. Chen, L. Zhang, et al., "Reserve margin enhancement of renewable energy in fundamental frequency regulation of the power grid," Energies, vol. 19, 718, 2026, doi: 10.3390/en19030718.
[17] X. Zhao, H. Hu, G. Shang, et al., "A collaborative wind-power storage system for primary frequency regulation considering wind-turbine rotational kinetic energy recovery," Energies, vol. 19, 658, 2026, doi: 10.3390/en19030658.
[18] X. Y. Zhang and J. F. Hu, "Virtual inertia request and collaborative assistance from the wind-storage integrated system," Trans. China Electrotech. Soc., vol. 39, pp. 672–685, 2024, doi: 10.13334/j.0258-8013.pcsee.230479.
[19] F. F. Miao and X. S. Tang, "Investigation of frequency behaviour of electric networks under wind-power and energy storage joint control," High Volt. Eng., vol. 41, pp. 2209–2216, 2015, doi: 10.13336/j.1003-6520.hve.2015.07.013.
[20] Wind Power in Power Systems. Hoboken, NJ, USA: John Wiley and Sons, 2012.